

Heterogeneous Catalysis

International Edition: DOI: 10.1002/anie.201704758
German Edition: DOI: 10.1002/ange.201704758

Integrated In Situ Characterization of a Molten Salt Catalyst Surface: Evidence of Sodium Peroxide and Hydroxyl Radical Formation

Kazuhiro Takanabe,* Abdulaziz M. Khan, Yu Tang, Luan Nguyen, Ahmed Ziani, Benjamin W. Jacobs, Ayman M. Elbaz, S. Mani Sarathy, and Franklin (Feng) Tao

Abstract: Sodium-based catalysts (such as Na_2WO_4) were proposed to selectively catalyze OH radical formation from H_2O and O_2 at high temperatures. This reaction may proceed on molten salt state surfaces owing to the lower melting point of the used Na salts compared to the reaction temperature. This study provides direct evidence of the molten salt state of Na_2WO_4 , which can form OH radicals, using in situ techniques including X-ray diffraction (XRD), scanning transmission electron microscopy (STEM), laser induced fluorescence (LIF) spectrometry, and ambient-pressure X-ray photoelectron spectroscopy (AP-XPS). As a result, Na_2O_2 species, which were hypothesized to be responsible for the formation of OH radicals, have been identified on the outer surfaces at temperatures of $\geq 800^\circ\text{C}$, and these species are useful for various gas-phase hydrocarbon reactions, including the selective transformation of methane to ethane.

Gas-phase radical chemistry involving OH radicals plays a crucial role in the oxidative coupling of methane (OCM),^[1] the dehydrogenation of ethane,^[2] atmospheric chemistry,^[3] and combustion reactions.^[4] The catalytic generation of OH radicals from O_2 and H_2O can occur on Pt metal and alkali earth oxides at high temperatures ($> 700^\circ\text{C}$).^[5] Alkaline metal containing catalysts (that is, Na supported on oxide) enhanced the rate of H_2O activation in the presence of O_2 and enhanced both the CH_4 conversion rate and C_2 selectivity during OCM.^[1] Otsuka et al. demonstrated that Na_2O_2 reacts with CH_4 to form methyl radicals at relatively low temperatures.^[6] Recently, kinetic evidence suggests that H_2O is

involved in the activation of CH_4 via the quasi-equilibrated formation of OH radicals when a Na-containing catalyst is used.^[1] In a similar context, an in situ Raman spectroscopic study identified Ba species on MgO that formed peroxide ions and was proposed as the active sites.^[7] However, direct evidence of the formation of this sodium peroxide species and an OH radical product are lacking. Here, in situ studies performed at high temperatures using different in situ characterization techniques were performed to identify the authentic active species during catalysis responsible for the OCM reaction. We report evidence for the formation of Na_2O_2 and OH radicals during the catalysis, and these species play a significant role in high-temperature gas-phase chemistry.

A detailed kinetic investigation that was focused on the effects of H_2O on the CH_4/O_2 reaction was reported in our previous studies.^[1] Briefly, the kinetic expression for the CH_4/O_2 reaction on Na-based catalysts at low conversion levels is given in (1):

$$r = r_{\text{O}^*} + r_{\text{OH}} = k'P_{\text{CH}_4}P_{\text{O}_2}^{0.5} + k''P_{\text{CH}_4}P_{\text{CH}_4}P_{\text{O}_2}^{0.25}P_{\text{H}_2\text{O}}^{0.5} \quad (1)$$

The first term corresponds to CH_4 activation via surface O^* (O^*), which is quasi-equilibrated with gas-phase O_2 (dry condition). The second term corresponds to CH_4 activation via an OH radical that is formed from O_2 and H_2O in quasi-equilibrated steps (wet condition). Among the studied catalysts, the $\text{Na}_2\text{WO}_4/\text{SiO}_2$ catalyst exhibited the highest contribution from the OH radical pathway relative to the surface O^* pathway as well as the highest selectivity to C_2

[*] Prof. K. Takanabe, A. M. Khan, Dr. A. Ziani
King Abdullah University of Science and Technology (KAUST)
KAUST Catalysis Center (KCC) and Physical Sciences and
Engineering Division (PSE)
4700 KAUST, Thuwal, 23955-6900 (Saudi Arabia)
E-mail: kazuhiro.takanabe@kaust.edu.sa
Y. Tang, Dr. L. Nguyen, Prof. F. Tao
Department of Chemical and Petroleum Engineering
Department of Chemistry, University of Kansas
Lawrence, KS 66045 (USA)
Dr. B. W. Jacobs
Protochips, Inc.
3800 Gateway Centre Blvd #306, Morrisville, NC 27560 (USA)
and
Analytical Instrumentation Facility, Materials Science and
Engineering Department, North Carolina State University
2410 Campus Shore Dr, Raleigh, NC 27695 (USA)
Dr. A. M. Elbaz, Prof. S. M. Sarathy
King Abdullah University of Science and Technology (KAUST)
Clean Combustion Research Center (CCRC) and

Physical Sciences and Engineering Division (PSE)
4700 KAUST, Thuwal, 23955-6900 (Saudi Arabia)

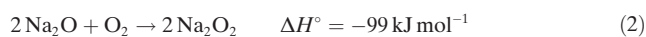
Dr. A. M. Elbaz
Mechanical Power Engineering Department
Faculty of Engineering Mataria, Helwan University
Al Sikka Al Hadid Al Gharbeya, Al Masaken Al Iqtisadeyah
Qism Helwan, Cairo Governorate (Egypt)

Supporting information (catalyst preparation, catalytic testing, characterization) and the ORCID identification number(s) for the author(s) of this article can be found under:
<https://doi.org/10.1002/anie.201704758>.

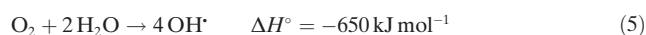
© 2017 The Authors. Published by Wiley-VCH Verlag GmbH & Co. KGaA. This is an open access article under the terms of the Creative Commons Attribution Non-Commercial NoDerivs License, which permits use and distribution in any medium, provided the original work is properly cited, the use is non-commercial, and no modifications or adaptations are made.

hydrocarbons from CH_4 .^[1d]

In this study, the TiO_2 support was chosen to replace SiO_2 to immobilize Na_2WO_4 and avoid charging effect during characterization using TEM and AP-XPS. The extensive heat treatment at 900°C for 15 h in flowing air ($100\text{ cm}^3\text{ min}^{-1}$) was essential to ensure the stability of the catalyst during OCM. In this process, the excess Na_2WO_4 was evaporated. The resulting Na contents in the SiO_2 and TiO_2 samples, which were measured using inductively coupled plasma, were about 4 and about 0.6 wt%, respectively, and these values did not change after the OCM kinetic testing at 800°C . The BET surface areas that were estimated by N_2 sorption were 2 and $3\text{ m}^2\text{ g}^{-1}$ for $\text{Na}_2\text{WO}_4/\text{SiO}_2$ and $\text{Na}_2\text{WO}_4/\text{TiO}_2$, respectively. In our studies, we confirmed that kinetic expression (1) applies to the $\text{Na}_2\text{WO}_4/\text{TiO}_2$ catalyst, which is consistent with the data reported for the $\text{Na}_2\text{WO}_4/\text{SiO}_2$ catalyst.^[1] The $\text{Na}_2\text{WO}_4/\text{TiO}_2$ catalyst exhibits excellent OCM selectivity in the presence of an $\text{O}_2/\text{H}_2\text{O}$ mixture and the catalyst most likely has the ability to form OH radicals from an O_2 and H_2O mixture. The details of the kinetic results are described in the Supporting Information, Figures S2. The proposed catalytic formation of OH radicals on the Na catalyst is as in (2)–(4).^[2,4]



Herein, H_2O and H_2O_2 can be gas-phase species or adsorbed species on the surface, even though gas-phase H_2O_2 (or decomposed product) is most likely present because its boiling point is 150°C . The Na_2O_2 decomposition temperature is 657°C , which may remain kinetically formed in the presence of O_2 . The overall reaction for the OH radical formation (when quasi-equilibrated in the gas phase) is according to (5):



Direct detection of OH radicals was attempted using a LIF spectrometer with the setup described in the Supporting Information, Figure S1. Owing to the detection limitations of our system, a transient condition was applied for the detection of OH radicals. The catalyst, which was placed in an alumina boat, was initially heated to 900°C under vacuum ($<1\text{ Pa}$), followed by the introduction of 2.3 kPa of H_2O into the system. As the 20 kPa of O_2 was gradually introduced into the heated reactor with the catalyst, the change in the LIF signal was successively recorded. Figure 1 shows the resulting transient detection of OH radicals. The OH radicals were detected upon introduction of an O_2 and H_2O mixture at 900 and 950°C , which is consistent with reaction (5). This result unambiguously confirms that the Na catalyst can form OH radicals from an O_2 and H_2O mixture. To the best of our knowledge, this result is the first evidence for the direct detection of OH radicals from an O_2 and H_2O mixture on a Na-based catalyst surface.

It is important to note that the melting point of Na_2WO_4 (698°C) is lower than the typical reaction temperature for the

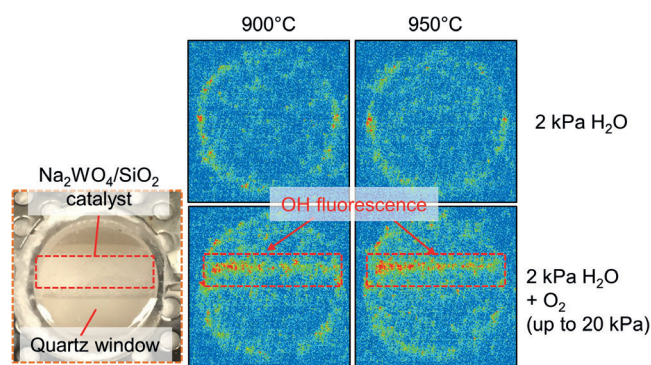


Figure 1. Detection of OH radicals through a quartz window using LIF spectroscopy. The setup details are provided in the Supporting Information.

CH_4 reaction ($\geq 800^\circ\text{C}$). Therefore, we attempted to capture the change of crystal structure and surface morphology using in situ XRD and TEM at high temperature in air. Figure 2a shows the XRD patterns of $\text{Na}_2\text{WO}_4/\text{TiO}_2$ collected at 500 – 800°C in flowing air. When the temperature was increased from 500 to 700°C , the XRD peaks for Na_2WO_4 disappeared, which suggests the formation of its molten salt state. Exposure to ambient air/moisture at room temperature resulted in recovery of the original phase (that is, cubic Na_2WO_4 ; the top XRD pattern of sample cooled down to 25°C in Figure 2a). This in situ XRD result (see also the Supporting Information, Figure S3) is consistent with the in situ Raman spectroscopy

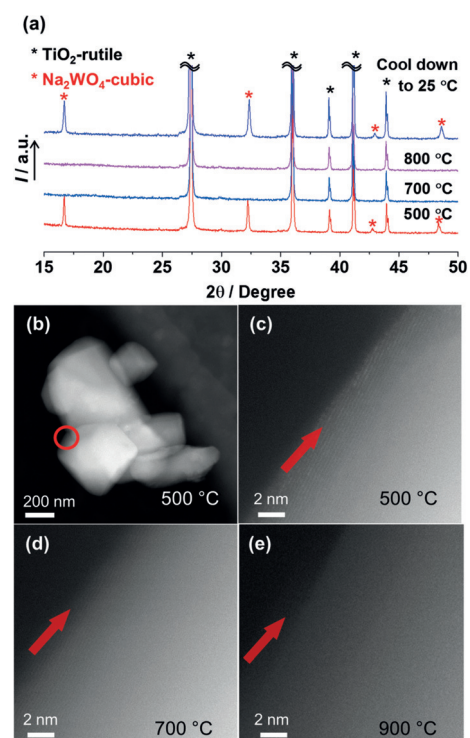


Figure 2. a) XRD patterns and b)–e) HAADF-STEM images for the $\text{Na}_2\text{WO}_4/\text{TiO}_2$ catalyst at different temperatures in the presence of air. b) Low magnification measured at 500°C ; high magnification at point in the circle in (b) measured at c) 500°C , d) 700°C , e) 900°C .

data reported by Yu et al., which confirms the disappearance of characteristic Raman peaks for Na_2WO_4 (supported on CeO_2) at high temperature.^[8] Our sample shows very small Raman peak ascribable to Na_2WO_4 owing to its low loading, as shown in the Supporting Information, Figure S4. The fusion temperature coincided with endothermic/exothermic behaviors for the differential scanning calorimetric measurement of the Na_2WO_4 salt during heating/cooling (Supporting Information, Figure S5).

Figure 2b–e also shows in situ the high-angle annular dark field (HAADF)-STEM images that were recorded at different temperatures (500–900 °C) in the presence of air. The sample pretreated at 900 °C exhibited a TiO_2 surface that was uniformly covered with a Na_2WO_4 film, as previously proposed by Lunsford et al. using ion scattering spectroscopy.^[8] At 700 °C or higher, the salt-covered surface becomes blurry as the *z*-contrast is weakened in the images (Figure 2d), which is indicative of salt melting. At 900 °C, the surface layer seems to disappear and the facet feature of the support surface (TiO_2) becomes more evident, owing to the absence of lattice of the melted salt, as shown in Figure 2e. Nevertheless, the energy dispersive spectroscopy (EDS) image confirmed the homogeneous distribution of Na and W species after the 800 °C treatment (Supporting Information, Figure S6).

The surface states of the $\text{Na}_2\text{WO}_4/\text{TiO}_2$ catalyst under different gas atmospheres ($\text{O}_2 + \text{H}_2\text{O}$ or $\text{O}_2 + \text{CH}_4$) at 800 °C were investigated using the AP-XPS system using a flowing reaction cell built by the Tao group.^[9] Photoemission features of subshell electrons of surface atoms can be collected when the catalyst is heated up to 850 °C in a flowing gas. The Na 1s, O 1s, and W 4f features of the catalyst in UHV and different gas atmospheres at different temperatures are shown in Figure 3. The binding energies of these spectra were calibrated to $\text{Au } 4f_{7/2}$ of Au foil, which was used to support the $\text{Na}_2\text{WO}_4/\text{TiO}_2$ catalyst particles (Supporting Information, Figure S7). As shown in Figure 3, the O 1s peak of the catalyst surface in UHV at 20 °C was located at 530.6 eV, which is consistent with the reported value.^[10] The W 4f_{7/2} peak can be identified even though W 4f_{5/2} overlaps with Ti 2p, as shown in Figure 3c and f. In UHV, W 4f_{7/2} was located at 36.0 eV, which is in good agreement with the

literature.^[10] The peak intensity of Na 1s was located at 1072.0 eV, which corresponds to Na 1s of Na_2WO_4 and is consistent with the reported value.^[11] To explore the surface state of Na_2WO_4 in the OH radical generation condition at 800 °C, a mixture of O_2 and H_2O was introduced into the flowing reaction cell for AP-XPS.^[10] The presence of free-state O_2 and H_2O gases was confirmed based on the observation of the photoemission features of the O 1s peaks (pink and blue line in Figure 3b and red line in Figure 3e) because they appear at a relatively higher binding energy than those of adsorbed species by a few eV. The peak positions at 539.1 and 535.8 eV were assigned to O_2 and H_2O in the gas phase, respectively, and are consistent with the references.^[12] The results provide strong evidence for the existence of gas environment around the catalyst. Intriguingly, the photoemission feature of Na 1s of the catalyst in a mixture of O_2 and H_2O at 800 °C upshifted by 1.0 eV, in contrast to that in a mixture of O_2 and H_2O at 20 °C (Figure 3d). This shift does not result from surface charging because there is no shift in W 4f_{7/2}. This upshift suggests a definite change in the chemical environment of the Na cations after being heated from 20 to 800 °C in a mixture of O_2 and H_2O . The high-binding energy peak at 1073.2 eV for Na 1s at 800 °C was assigned to peroxide species (that is, Na_2O_2), which is consistent with the observed binding energy of Na 1s of Na_2O_2 reported previously.^[13]

To check the authentic chemical state of the Na_2WO_4 catalyst during OCM catalysis at 800 °C, O_2 and CH_4 were mixed and then introduced to the reaction cell containing the Na_2WO_4 catalyst for AP-XPS. At room temperature in a mixture of O_2 and CH_4 , the photoemission features of Na 1s, O 1s, and W 4f (blue lines in Figure 3a–c) are the same as those in UHV at 20 °C (black lines in Figures 3d–f), except for the observation of an O 1s peak of gaseous O_2 . By heating the sample to 800 °C by an infrared laser beam and maintaining the catalyst at 800 °C in a mixture of O_2 and CH_4 during AP-XPS data acquisition,^[10] Na 1s with a binding energy at 1073.1 eV was observed during catalysis. Notably, the photoemission feature of Na 1s of the surface of the catalyst during catalysis (pink line in Figure 3a) is very similar to that observed at 800 °C in a mixture of O_2 and H_2O (red line in Figure 3d). Clearly, the AP-XPS studies of nominal catalyst Na_2WO_4 supported on TiO_2 during OCM at 800 °C uncovered that the authentic surface phase of the Na species during catalysis was in fact Na_2O_2 . Therefore, this result was due to the quasi-equilibrated generation of Na_2O_2 in the presence of O_2 under the studied conditions.^[13]

The formation of Na_2O_2 is consistent with the quantitative analysis of the photoemission features collected under ($\text{O}_2 + \text{H}_2\text{O}$) and ($\text{O}_2 + \text{CH}_4$) atmospheres. As shown in Figure 4a (data are normalized to the ratio in UHV at 20 °C), the relative ratios of Na 1s to O 1s at 800 °C was higher than those at 20 °C. This result is consistent with the higher Na to O stoichiometric ratio in Na_2O_2 (1:1) than Na_2WO_4 (2:1). The peaks centered at 36.3 eV (W 4f_{7/2}) and at 38.0 eV (W 4f_{5/2} and Ti 3p) were deconvoluted to obtain the relative area ratios of Na 1s and W 4f_{7/2}, and the results are plotted in Figure 4b (data are normalized to the ratio in UHV at 20 °C). Notably, the Na 1s/W 4f_{7/2} area ratios under ($\text{O}_2 + \text{H}_2\text{O}$) or ($\text{O}_2 + \text{CH}_4$) were relatively increased from 20 to 800 °C. These

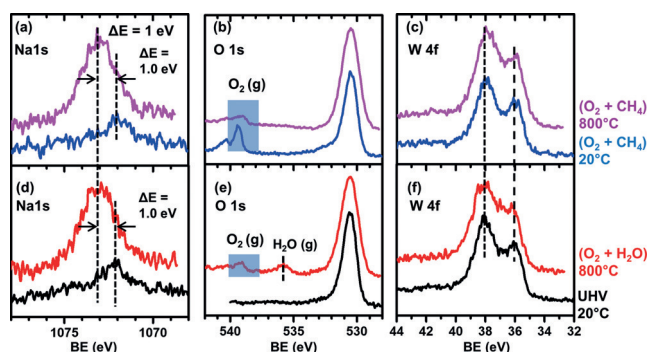


Figure 3. Photoemission features of Na 1s, O 1s, and W 4f for the catalyst collected at UHV, 20 °C (black line), 66 Pa O_2 and 66 Pa H_2O at 800 °C (red line), 66 Pa O_2 and 66 Pa CH_4 at 20 °C (blue line), and 66 Pa O_2 and 66 Pa CH_4 at 800 °C (pink line).

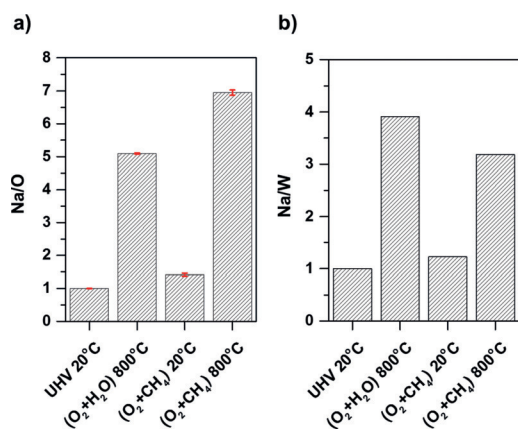


Figure 4. Area ratios of a) Na 1s/O 1s and b) Na 1s/W 4f_{7/2} of the catalyst surface at 800 °C in a mixture of 66 Pa O₂ and 66 Pa H₂O; and at 20 and 800 °C in a mixture of 66 Pa CH₄ and 66 Pa O₂, relative to the ratios obtained at 20 °C in UHV.

increases suggest that the molten salt film became richer in sodium cations on the outer surface and lean in W atoms on the topmost surface layers. These quantitative analyses of the surface composition of nominal Na₂WO₄ obtained during catalysis suggest the formation of Na₂O₂ layers on top of the surface, which blocks the photoelectrons of W 4f of Na₂WO₄ from escaping to travel to gas phase or UHV. Therefore, the Na/W ratio increased once the Na₂O₂ layer was formed. Thus, we can conclude that Na₂O₂ formed on the surface of Na₂WO₄ during catalysis and under the reaction conditions at 800 °C.

With regard to the OCM selectivity, the active site has been extensively discussed for Mn/Na₂WO₄/SiO₂ (or supported on other oxides).^[1,2,9,11,14] In our previous study,^[1d] we confirmed that Mn and W are not essential components for the selective OCM reaction. However, H₂O was identified as a key reactant (wet condition). In contrast, the supported Na₂WO₄ is a poor catalyst for the activation of CH₄. Mn is effective for mildly burning CH₄ to generate H₂O from a CH₄/O₂ mixture (dry condition), which is taken over by the OH radical pathway at high conversions (leading to the wet condition). WO₄ anions are most likely effective at immobilizing Na cations, which otherwise would sublime easily (NaOH: m.p. 318 °C, b.p. 1388 °C, Na₂WO₄: m.p. 698 °C). The support material should be inert and accommodate the Na₂WO₄ liquid film on its surface at high temperature,^[8] and the topmost layer becomes Na₂O₂, which was observed by AP-XPS.

In conclusion, in situ spectroscopic and microscopic techniques were employed for identifying the authentic species of the Na-based catalyst at 800 °C under OCM relevant conditions. The catalyst was active for generation of OH radicals from O₂ and H₂O at high temperature, as measured by OH radical selective LIF spectroscopy. The molten salt state of Na₂WO₄ on oxides at high temperature was confirmed using in situ XRD measurements and STEM images performed at high temperature. The in situ studies using AP-XPS clearly uncovered the formation of Na₂O₂ under reaction conditions at high temperature (ca. 800 °C),

which is considered to be responsible for OH radical formation. The specific binding energy of Na 1s and the increased Na/W atomic ratio during catalysis at 800 °C revealed a surface that is richer in newly formed Na₂O₂. This study provides an excellent demonstration of integration of in situ electron spectroscopic and in situ electron microscopic techniques in identifying authentic surface phase of a nominal catalyst during catalysis at high temperatures in a mixture consisting of all the reactants of a catalytic reaction.

Acknowledgements

The research reported in this study was supported by the King Abdullah University of Science and Technology (KAUST). A part of the work was also financially supported by the U.S. Department of Energy, Office of Science, Office of Basic Energy Sciences, Chemical Sciences, Geosciences and Biosciences Division under Award Number DE-SC0014561. Both instrumentation of the second lab-based AP-XPS system and the design of high temperature AP-XPS reaction cell were supported through the fund of the U.S. Department of Energy, Office of Science, Office of Basic Energy Sciences, Chemical Sciences, Geosciences, and Biosciences Division under Award (DE-SC0014561). L.N. was partially supported by KAUST. Y.T. and F.T. were supported by the DOE Award (DE-SC0014561).

Conflict of interest

The authors declare no conflict of interest.

Keywords: ambient-pressure XPS · heterogeneous catalysis · hydroxyl radicals · oxidative coupling · sodium peroxide

How to cite: *Angew. Chem. Int. Ed.* **2017**, *56*, 10403–10407
Angew. Chem. **2017**, *129*, 10539–10543

- [1] a) K. Takanaabe, E. Iglesia, *Angew. Chem. Int. Ed.* **2008**, *47*, 7689–7693; *Angew. Chem.* **2008**, *120*, 7803–7807; b) K. Takanaabe, E. Iglesia, *J. Phys. Chem. C* **2009**, *113*, 10131–10145; c) K. Takanaabe, *J. Jpn. Pet. Inst.* **2012**, *55*, 1–12; d) Y. Liang, Z. Li, M. Nouridine, S. Shahid, K. Takanaabe, *ChemCatChem* **2014**, *6*, 1245–1251.
- [2] K. Takanaabe, S. Shahid, *AICChE J.* **2017**, *63*, 105–110.
- [3] a) H. Levy II, *Science* **1971**, *173*, 141–143; b) P. K. Patra, M. C. Krol, S. A. Montzka, T. Arnold, E. L. Atlas, et al., *Nature* **2014**, *513*, 219–223.
- [4] a) C. K. Westbrook, *Proc. Combust. Inst.* **2000**, *28*, 1563–1577; b) M. Blocquet, C. Schoemaeker, D. Amedro, O. Herbinet, F. Battin-Leclerc, C. Fittschen, *Proc. Natl. Acad. Sci. USA* **2013**, *110*, 20014–20017.
- [5] a) L. C. Anderson, M. Xu, C. E. Mooney, M. P. Rosynek, J. H. Lunsford, *J. Am. Chem. Soc.* **1993**, *115*, 6322–6326; b) K. B. Hewett, L. C. Anderson, M. P. Rosynek, J. H. Lunsford, *J. Am. Chem. Soc.* **1996**, *118*, 6992–6997; c) K. B. Hewett, M. P. Rosynek, J. M. Lunsford, *Catal. Lett.* **1997**, *45*, 125–128; d) S. Noda, M. Nishioka, A. Harano, M. Sadakata, *J. Phys. Chem. B* **1998**, *102*, 3185–3191.
- [6] K. Otsuka, A. A. Said, K. Jinno, T. Komatsu, *Chem. Lett.* **1987**, 77–80.

- [7] J. H. Lunsford, X. Yang, K. Haller, J. Laane, G. Mestl, H. Knözinger, *J. Phys. Chem.* **1993**, *97*, 13810–13813.
- [8] Z. Yu, X. Yang, J. H. Lunsford, M. P. Rosynek, *J. Catal.* **1995**, *154*, 163–173.
- [9] L. Nguyen, F. Tao, *Rev. Sci. Instrum.* **2016**, *87*, 064101.
- [10] Z.-C. Jiang, C.-J. Yu, X.-P. Fang, S.-B. Li, H.-L. Wang, *J. Phys. Chem.* **1993**, *97*, 12870–12875.
- [11] T. W. Elkins, H. E. Hagelin-Weaver, *Appl. Catal. A* **2015**, *497*, 96–106.
- [12] a) B. Eren, C. Heine, H. Bluhm, G. A. Somorjai, M. Salmeron, *J. Am. Chem. Soc.* **2015**, *137*, 11186–11190; b) J. T. Newberg, D. E. Starr, S. Yamamoto, S. Kaya, T. Kendelewicz, E. R. Mysak, S. Porsgaard, M. B. Salmeron, G. E. Brown, A. Nilsson, *Surf. Sci.* **2011**, *605*, 89–94; c) S. Yamamoto, T. Kendelewicz, J. T. Newberg, G. Ketteler, D. E. Starr, E. R. Mysak, K. J. Andersson, H. Ogasawara, H. Bluhm, M. Salmeron, G. E. Brown, Jr., A. Nilsson, *J. Phys. Chem. C* **2010**, *114*, 2256–2266.
- [13] Q.-H. Wu, A. Thißen, W. Jaegermann, *Appl. Surf. Sci.* **2005**, *252*, 1801–1805.
- [14] a) X. Fang, S. Li, J. Lin, J. Gu, D. Yang, *J. Mol. Catal.* **1992**, *6*, 427; b) D. Wang, M. P. Rosynek, J. H. Lunsford, *J. Catal.* **1995**, *155*, 390–402; c) A. Palermo, J. P. H. Vazquez, A. F. Lee, M. S. Tikhov, R. M. Lambert, *J. Catal.* **1998**, *177*, 259–266; d) S. Pak, P. Qiu, J. H. Lunsford, *J. Catal.* **1998**, *179*, 222–230; e) S. Pak, J. H. Lunsford, *Appl. Catal. A* **1998**, *168*, 131–137; f) A. Palermo, J. P. H. Vazquez, R. M. Lambert, *Catal. Lett.* **2000**, *68*, 191–196; g) S. Ji, T. Xiao, S. Li, L. Chou, B. Zhang, C. Xu, R. Hou, A. P. E. York, M. L. H. Green, *J. Catal.* **2003**, *220*, 47–56; h) S. Hou, Y. Cao, W. Xiong, H. Liu, Y. Kou, *Ind. Eng. Chem. Res.* **2006**, *45*, 7077–7083; i) M. R. Lee, M.-J. Park, W. Jeon, J.-W. Choi, Y. W. Suh, D. J. Suh, *Fuel Process. Technol.* **2012**, *96*, 175–182; j) S. Arndt, T. Otremba, U. Simon, M. Yildiz, H. Schubert, R. Schomäcker, *Appl. Catal. A* **2012**, *425–426*, 53–61; k) V. Lomonosov, Y. Gordienko, M. Sinev, *Top. Catal.* **2013**, *56*, 1858–1866; T. Serres, C. Aquino, C. Mirodatos, Y. Schuurman, *Appl. Catal. A* **2015**, *504*, 509–518.

Manuscript received: May 9, 2017

Revised manuscript received: June 19, 2017

Accepted manuscript online: June 26, 2017

Version of record online: July 24, 2017